

Do atmospheric aerosols form glasses?

(accepted for publication in ACP)

B. Zobrist^{1,2}, C. Marcolli¹, D. A. Pedernera² and T. Koop²

Contact: bernhard.zobrist@env.ethz.ch

¹Institute for Atmospheric and Climate Science, ETH Zurich, Zurich, Switzerland; ²Department of Chemistry, Bielefeld University, Bielefeld, Germany

Introduction:

What is a glass:

- Glasses are amorphous (non-crystalline) materials that behave mechanically as solids
- Produced by cooling or by a liquid without crystallization
- Extremely high viscosities, @ the glass temperature, T_g , $\approx 10^{12}$ Pa s, (honey ≈ 2 Pa s)
- Extremely low molecular diffusion, $D_{H_2O} \approx 10^{-20} \text{ m}^2 \text{ s}^{-1}$, which implies that a water molecule would need more than a day (Δt) to diffuse into a 50 nm (Δx) aerosol particle:

$$\Delta t = \frac{(\Delta x)^2}{D_{H_2O}} = \frac{(50 \cdot 10^{-9} \text{ m})^2}{10^{-20} \text{ m}^2 \text{ s}^{-1}} = 2.5 \cdot 10^5 \text{ s} \geq 1 \text{ day}$$

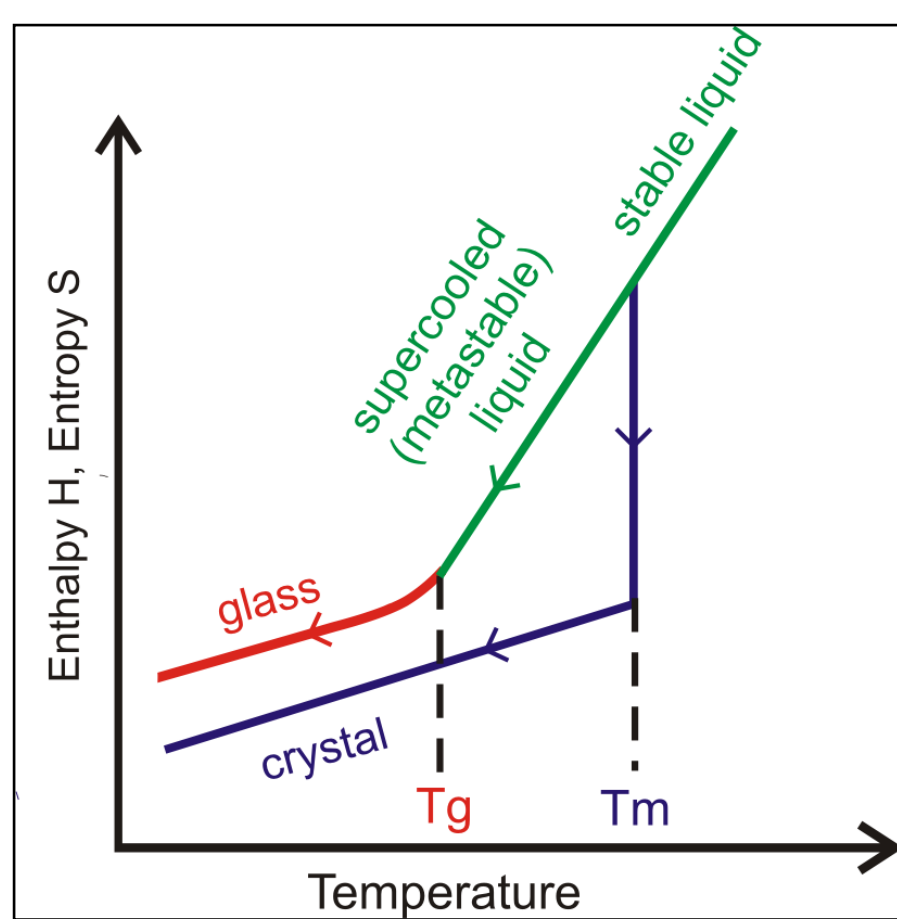


Fig. 1. Enthalpy and entropy change during the phase transitions of a crystallization/melting (first order phase change) and a glass transition.

If aqueous aerosols form glasses, then inhibition of:

- Water uptake
- Chemical reactions
- Crystal growth (e.g., ice)
- Ice nucleation

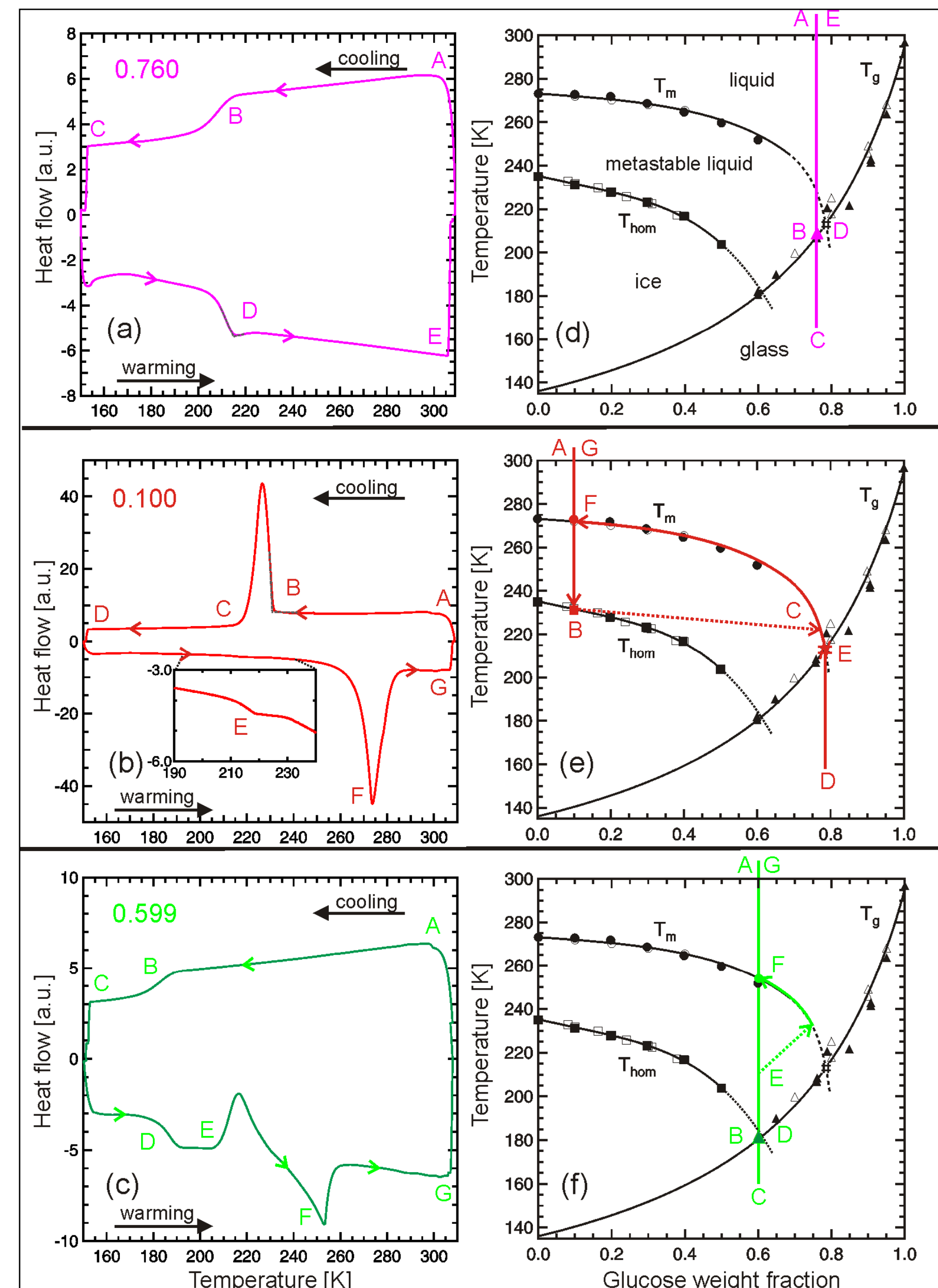


Fig. 2. DSC thermograms, panels (a)–(c), and state diagrams, panels (d)–(f), of 3 different concentrated aqueous glucose solutions: 0.760, 0.100 and 0.599 weight fraction. Panels (a)–(c): cooling/heating cycles from 308 K to 153 K with 10Kmin⁻¹. Panels (d)–(f): The colored curves depict the course of the DSC experiments linked to the panel on the left side. Circles: T_m ; Squares: T_{hom} ; Triangles: T_g ; Hash: T_g' of the freeze concentrated solution.

Experimental investigations:

Glass temperatures, T_g , homogeneous ice freezing, T_{hom} , and ice melting temperatures, T_m , of emulsified and bulk samples made of various inorganic, organic and inorganic/organic aqueous solutions have been investigated with a differential scanning calorimeter (DSC), see Fig. 2.

Investigated solutes:

- Organics:** Polyols: 1,4-butanediol (C4, 90.1 gmol⁻¹); 2,5-hexanediol; 1,2,6-hexanetriol; 1,2,7,8-octanetetrol (C8); 2,2,6,6-Tetrakis(hydroxymethyl)cyclohexanol, C₁₀H₂₀O₅

Sugars/anhydrosugars: glucose; sucrose; raffinose (504.5 gmol⁻¹); levoglucosan

Various compounds: mixture of 5 dicarboxylic acids (M5); an aromatic compound (DL-4-Hydroxy-3-methoxy mandelic acid, (HMMA), C₉H₁₀O₅); glycerol

- Inorganics:** sulphuric acid, ammonium bisulphate, nitric acid, ammonium sulphate (AS) and ammonium nitrate (AN).

- Inorganic/organic mixtures:** mixture of M5 and AS (M5AS); 1:1 (by mass) mixtures of M5AS and raffinose, of C4 and C8 polyols and of glucose and AN

(model compounds of the water soluble organic fraction, Decesari et al. 2006; molar mass between 60–500 gmol⁻¹ are observed for organics in field studies e.g., Krivácsy et al. 2001)

Gordon-Taylor equation:

Glass curves as a function of the solute weight fraction can be calculated over the entire concentration range (see Figs 2 and 3), with:

$$T_g(w_2) = \frac{w_1 \cdot T_{g1} + \frac{1}{k} w_2 \cdot T_{g2}}{w_1 + \frac{1}{k} w_2} \quad (1)$$

where w_1 and w_2 are the solute weight fractions of water and the solute, T_{g1} and T_{g2} are the glass temperatures of water and the solute, respectively ($T_{g1} = 136$ K, Johari et al. 1987). The T_g data are then transformed from the weight fraction to the water activity scale (using water activity measurements, not shown here) leading to Figs. 4 and 5.

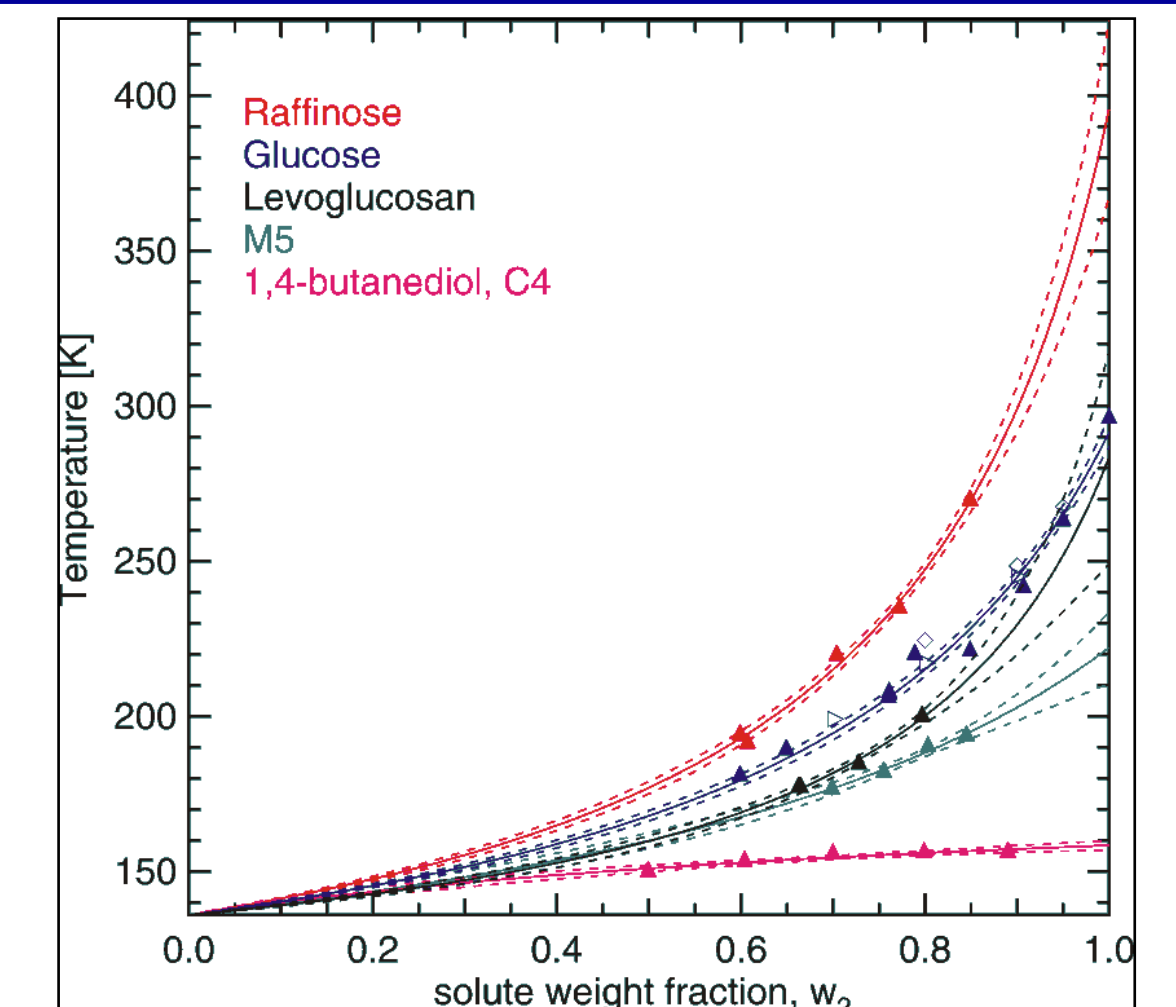


Fig. 3. Symbols: measurements; Solid lines: Glass curves for five selected solutes as a function of the solute weight fraction calculated with Eq. 1. Dashed lines: uncertainty range on a one standard deviation level for the solid lines.

Glass temperatures of organic and multi-component solutions:

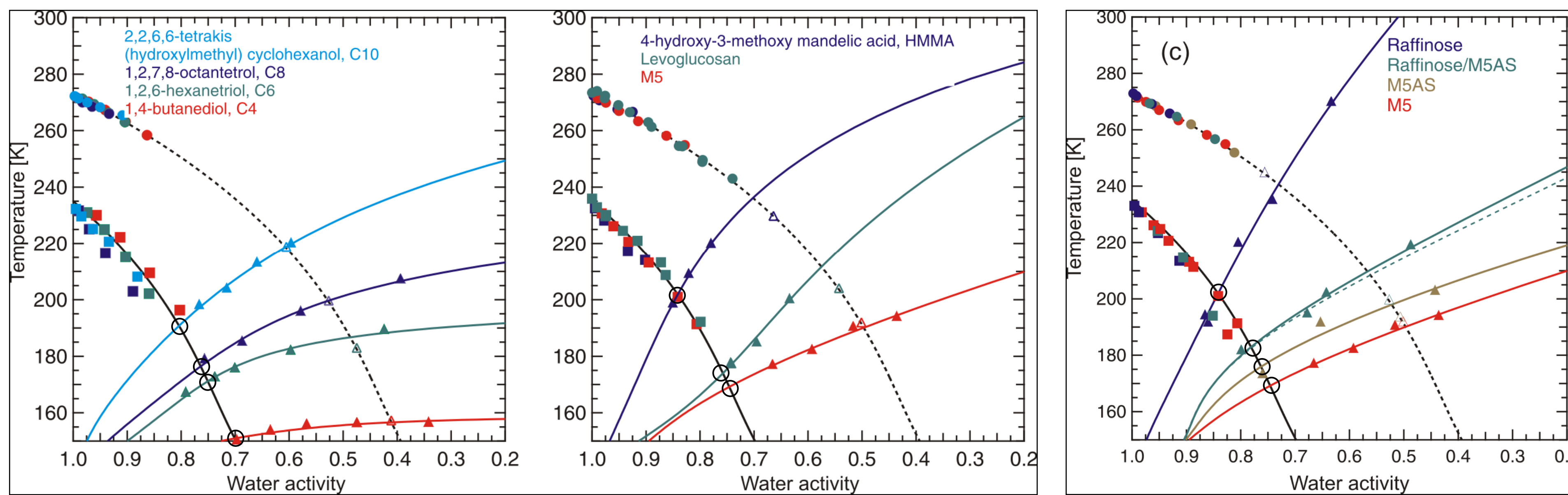


Fig. 4. State diagrams for several organic/water systems as a function of water activity, a_w . Circles: Ice melting temperatures, T_m ; squares: homogeneous ice freezing temperatures T_{hom} ; filled upward triangles and filled right pointed triangles: T_g' ; Solid lines: Glass curves; Dashed and solid black lines: Ice melting and homogeneous ice freezing curves, according to Koop et al. 2000, respectively. The large black circles denotes the T_g' for each solute, i.e., intersection between T_g and T_{hom} curves (see also Fig. 6)

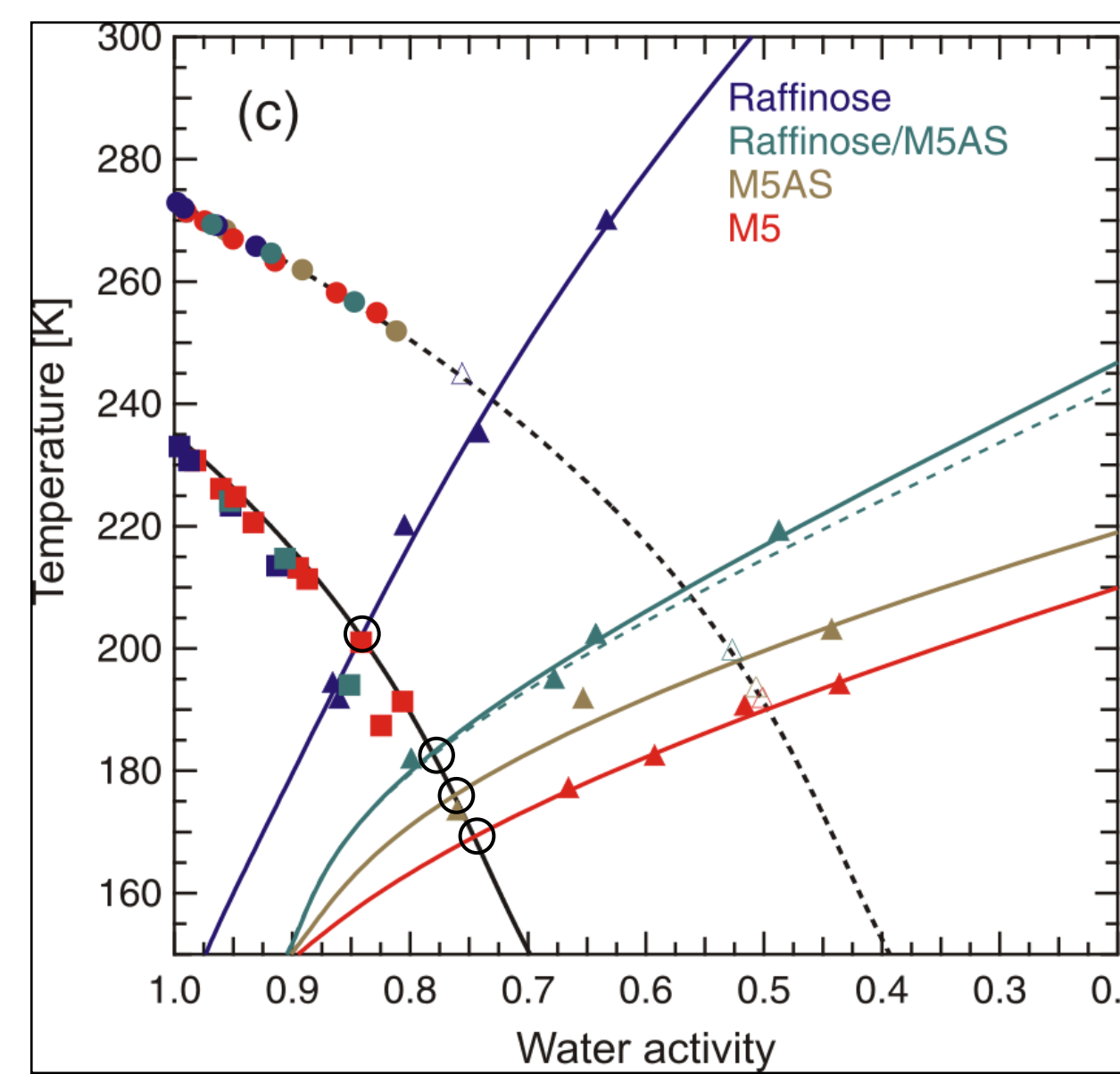


Fig. 5. State diagrams of multi-component solutions in the water activity scale. Circles: T_m ; squares: T_{hom} ; filled triangles: T_g ; open triangles: T_g' ; Solid colored curves: Glass curves. Black circles: see Fig. 4.

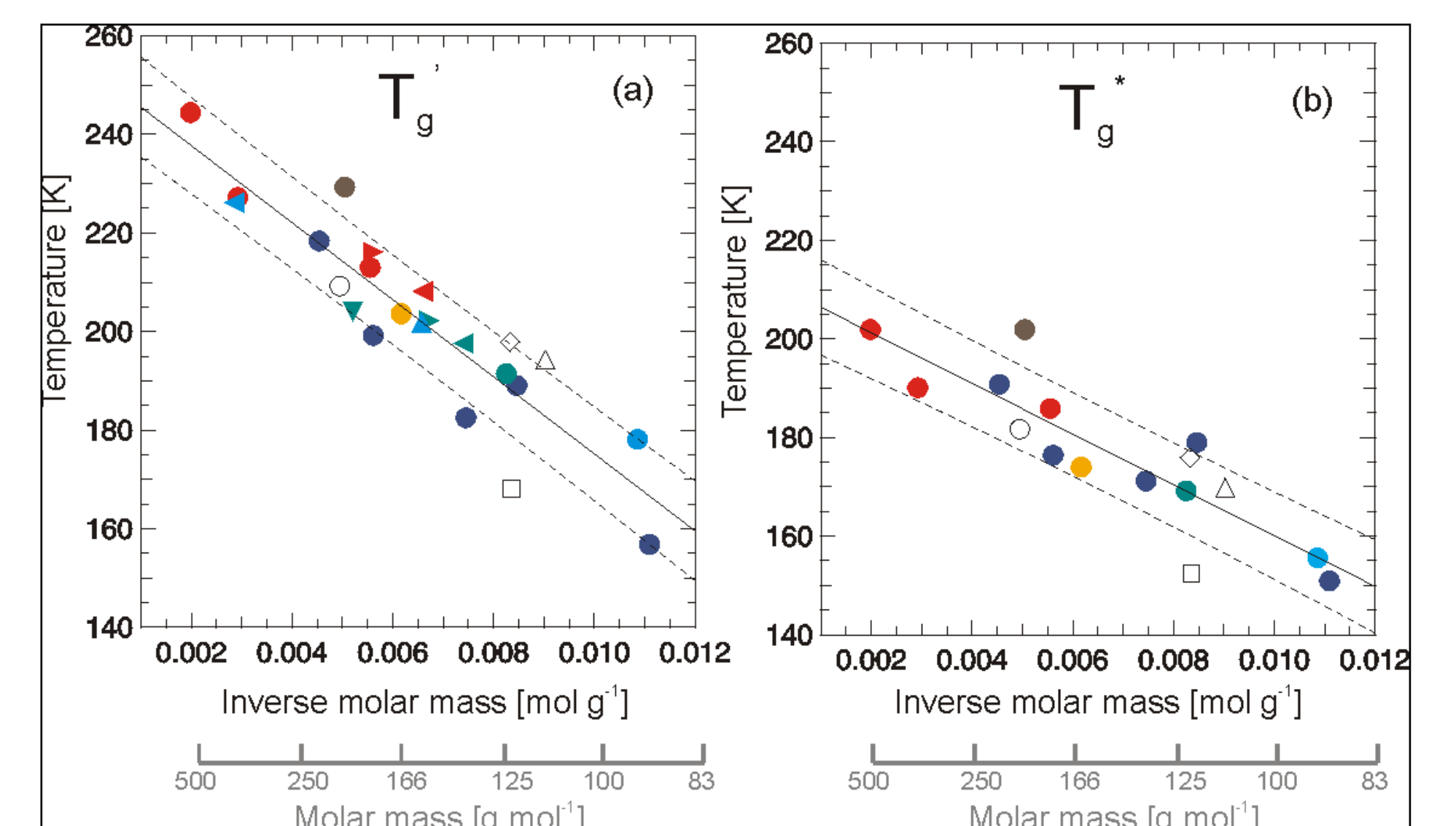


Fig. 6. T_g' , panel (a), and T_g^* , panel (b), for aqueous solutions as a function of the inverse molar mass of the solute. Filled and open symbols stand for aqueous organic and multi-component solutions, respectively. The colors of the filled symbols denote the different substances or compound classes. Red: sugars; blue: polyols; light blue: sugar alcohols; green: dicarboxylic acids; brown: HMMA; orange: levoglucosan. The open symbols are labelled as, circle: raffinose/M5AS, square: C4/C8, triangle: glucose/ NH_4NO_3 and diamond: M5AS. The figure contains some data points from the literature: Luyet and Rasmussen 1968; Roos 1993; Maltini et al. 1997 and Murray 2008.

Atmospheric implications:

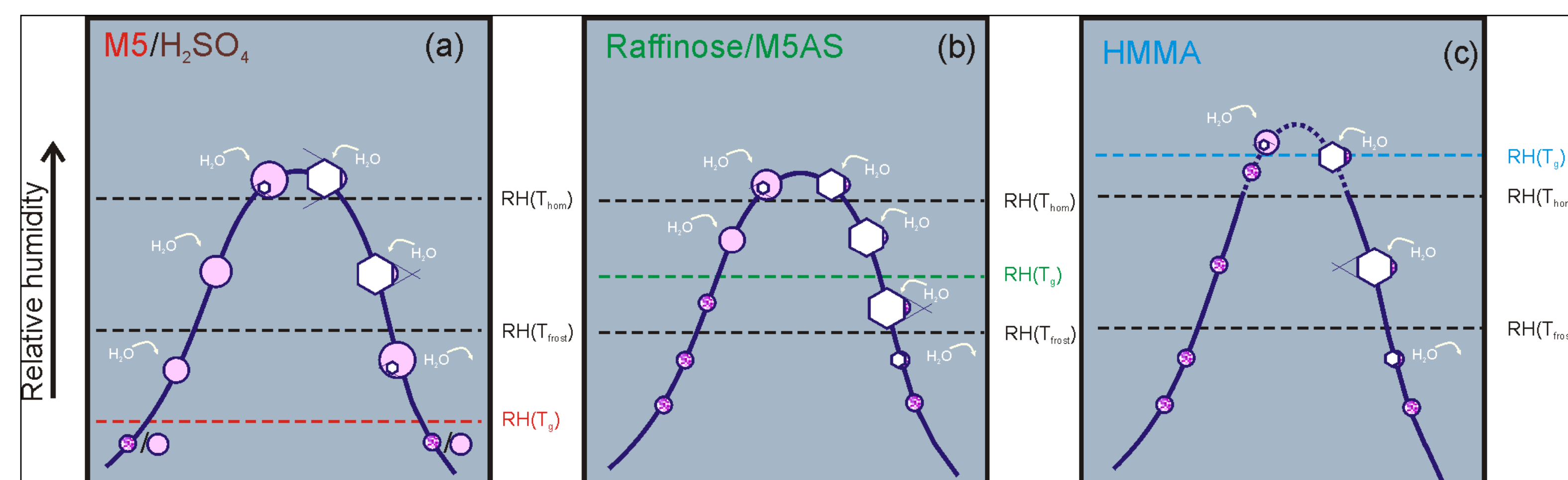


Fig. 7. (top) Schemes for the physical states of model aerosols following the trajectory on the left. Uniform-colored circles: liquid; Hexagon: ice; Spotted circles: glass. The white arrows denote the water exchange between the aerosol and the gas phase.

Fig. 8. (left) Typical atmospheric trajectory (dark blue curve with symbols) as a function of the equilibrium relative humidity of the air. Solid black and dashed black lines: T_{hom} and T_m curve. The black square and circle are the relative humidities at the homogeneous ice freezing point, $RH(T_{hom})$ and at the frost point $RH(T_{frost})$ of the trajectory, respectively. The colored triangles are the intersections of the trajectory with the glass curves, which are labeled as $RH(T_g)$ in Fig. 7.

Acknowledgements

We are grateful for support by the European Commission through the integrated project SCOUT-O3 and by the Swiss National Fund in various projects.

Conclusions and Outlook:

- Glass formation was observed in most of the investigated aqueous solutions (except AN and AS, cooling rate to low?) Gordon-Taylor can describe the measured T_g over the entire concentration range.
- It is unlikely that inorganic solutions form glasses under atmospheric conditions
- Aqueous organic and multi-component solutions undergo glass transitions important at atmospheric temperatures and relative humidities
- T_g of such solutions depend predominantly on the molar mass of the solutes with a larger molar mass leading to a higher T_g . To a lesser extent T_g also depends on the hydrophilicity of the molecules, with more hydrophobic molecules showing higher T_g .
- The T_g curves of the multi-component solutions are located between the T_g curves of the binary solutions closer to that binary system with the lower T_g .
- Chemical reactions are impeded in viscous aerosol particles and might be even inhibited completely in glassy aerosol particles. This may increase the lifetime of the aerosol with respect to chemical decomposition
- Water uptake is diminished or even fully inhibited for highly viscous or glassy aerosols, respectively.
- Ice nucleation is inhibited at the homogeneous ice nucleation threshold when the aerosol is in a glassy state which leads to higher ice supersaturations than expected for liquid aerosols, mostly for $T < 202$ K. Vitrification organic-enriched aerosols might lead to cirrus clouds with smaller ice particle number densities when compared to inorganic aerosols, which will influence the radiative effect of cirrus.
- Knowledge of the chemical composition of the UT must be improved
- Water uptake and chemical reactions will be investigated by modelling and experimental studies

References:

- Decesari, S. et al., Atmos. Chem. Phys., 6, 375–402, 2006; Johari, G. P., Hallbrucker, A., and Mayer, E., Nature, 330, 552–553, 1987; Koop, T., Luo, B. P., Tsias, A., and Peter, T., Nature, 406, 611–614, 2000; Krivácsy, Z. et al., J. Atmos. Chem., 39, 235–259, 2001. Luyet, B. and Rasmussen, D., Biodynamica, 10, 167–191, 1968. Maltini, E., Anese, M., and Shtylla, I., Cryoleters, 18, 263–268, 1997; Murray, B. J., Atmos. Chem. Phys. Discuss., 8, 8743–8771, 2008; Roos, Y. H., Carbohydr. Res., 238, 39–48, 1993.